Zeolite-Based Organized Molecular Assemblies. Photophysical Characterization and Documentation of Donor Oxidation upon Photosensitized Charge Separation

Anwar A. Bhuiyan and James R. Kincaid*

Chemistry Department, Marquette University, Milwaukee, Wisconsin 53201-1881

Received February 15, 2001

An organized molecular assembly composed of two ruthenium polypyridine complexes, $Ru(bpy)_2(bpz)^{2+}$ and $Ru(bpy)_2(H_2O)_2^{2+}$ (where bpy = 2, 2′-bipyridine and bpz = 2, 2′-bipyrazine), has been prepared in adjacent supercages of Y-zeolite. This material has been characterized by diffuse reflectance, electronic absorption, electronic emission, and resonance Raman (RR) spectroscopy, as well as lifetime measurements. The spectral results confirm the identity of the entrapped complexes and resonance Raman measurements show that the relative concentrations of the two complexes within the zeolite particles are identical. A dramatic decrease in emission intensity observed for the adjacent cage assembly, relative to that observed for an appropriate reference material composed of a mixture of zeolite particles containing the separated complexes, indicates strong interaction between the adjacent complexes which provides an additional nonradiative decay pathway. The excited state lifetime measurements implicate a very short-lived component, dominating the decay curve at early times, which is most reasonably attributed to excited-state electron-transfer quenching of the adjacent cage pair. More importantly, analysis of diffuse reflectance spectra acquired during selective (sensitizer) irradiation of a sample of this material, wherein the remaining cages are filled with a suitable acceptor (MV^{2+}), provides direct evidence for oxidation of the $Ru(bpy)_2(H_2O)_2^{2+}$ donor complex, confirming the targeted synergy of the adjacent cage assembly.

Introduction

Zeolites have long been exploited as supports or hosts for adsorbed or entrapped transition metal catalysts or photocatalysts.[1,2] These materials are aluminosilicates whose three-dimensional structure is made up of corner sharing SiO_4 and AlO_4 tetrahedra, with exchangeable cations (M^+) occupying extraframework positions to neutralize charge.[3] Y-zeolite, one of the most commonly encountered materials, possesses a framework which consists of so-called "supercages" of approximately 13 Å diameter, each of which is connected to four, tetrahedrally arranged, adjacent supercages by openings having 7−8 Å "windows". It is emphasized here that the four cages adjacent to a given central cage do not share a common window with each other; i.e., none of these four supercages are adjacent to one another. This is an important point in considering the systems to be discussed below.

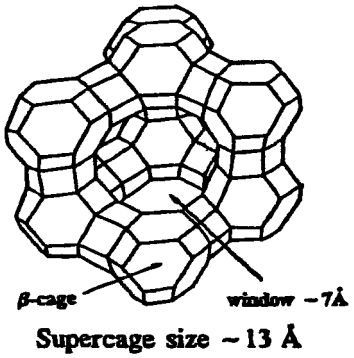

Following the pioneering work of Lunsford and co-workers,[4] which first demonstrated the feasibility of generating and entrapping the (12 Å) familiar photosensitizer,[5] $Ru(bpy)_3^{2+}$, within the supercages of zeolite-Y particles, Dutta and co-workers[6] reported an elegant series of studies which explored the utility of zeolite-entrapped $Ru(bpy)_3^{2+}$ for photoinduced charge separation. Specifically, these workers documented the formation of methyl viologen radicals upon irradiation of Ru-

(1) (a) Lunsford, J. H. ACS Symposium Series 40; American Chemical Society: Washington, DC, 1977; p 473. (b) Kalyanasundaram, K. *Photochemistry in Microheterogeneous Systems*; Academic Press: New York, 1987. (c) Ramamurthy, V., Ed. *Photochemistry in Organized and Constrained Media*; VCH: New York, 1991. (d) De Vos, D. E.; Knops-Gerrits, P. P.; Parton, R. F.; Weckhuysen, B. M.; Jacobs, P. A.; Schoonheydt, R. A. *J. Inclusion Phenom. Mol. Recogn. Chem.* **1995**, *21*, 185. (e) Bedoui, F. *Coord. Chem. Rev.* **1995**, *144*, 39.

(2) (a) Faulkner, L. R.; Suib, S. L.; Renschler, L. L.; Green, J. M.; Bross, P. R. In *Chemistry in energy production*; Wymer, R. G., Keller, O. L., Eds.; ACS Symposium Series 99; American Chemical Society: Washington, DC, 1982. (b) Li, Z.; Wang, C. H.; Persaud, L.; Mallouk, T. E. *J. Phys. Chem.* **1988**, *92*, 2592. (c) Kruger, J. S.; Mayer, J. A.; Mallouk, T. E. *J. Am. Chem. Soc.* **1988**, *110*, 8232. (d) Kim, Y.; Mallouk, T. E. *J. Phys. Chem.* **1992**, *96*, 2879. (e) Turbeville, W.; Robins, D. S.; Dutta P. K. *J. Phys. Chem.* **1992**, *96*, 5024.

(3) (a) Breck, D. W. *Zeolite Molecular Sieves: Structure Chemistry And Use*; Wiley: New York, 1974. (b) *Zeolite and Related Materials: State of the Art*; Weitcamp, J., Karge, H. G., Pfeifer, H., Holderich, W., Eds.; Elsevier: Amsterdam, 1994.

(4) (a) DeWilde, W.; Peeters, G.; Lunsford, J. H. *J. Phys. Chem.* **1980**, *84*, 2306. (b) Quayle, W. H.; Lunsford, J. H. *Inorg. Chem.* **1982**, *21*, 97.

(5) (a) *Photochemical Conversion and Storage of Solar Energy*; Norris, J. R., Jr., Meisel, D., Eds.; Elsevier: Amsterdam, 1988. (b) Kalyanasundaram, K. *Photochemistry of Polypyridine and Porpyhrin Complexes*; Academic Press: San Diego, 1992. (c) Juris, A.; Balzani, V.; Barigelletti, F.; Campagna, S.; Belser, P.; Von Zelewsky, A. *Coord. Chem. Rev.* **1988**, *84*, 85. (d) Meyer, T. J. *Acc. Chem. Res.* **1989**, *22*, 163. (e) Gratzel, M. *Acc. Chem. Res.* **1981**, *14*, 376. (f) Amouyal, E. *Sol. Energy Mater. Sol. Cells* **1995**, *38*, 249.

(6) (a) Dutta, P. K.; Incavo, J. A. *J. Phys. Chem.* **1987**, *91*, 4443. (b) Dutta, P. K.; Turbeville, W. *J. Phys. Chem.* **1992**, *96*, 9410. (c) Borja, M.; Dutta, P. K. *Nature* **1993**, *362*, 43. (d) Dutta, P. K.; Borja, M.; Ledney, M. *Sol. Energy Mater. Sol. Cells* **1995**, *38*, 239.

10.1021/ic010191m CCC: $20.00
Published on Web 07/19/2001

$(bpy)_3^{2+}$ loaded zeolite particles, wherein each of the remaining cages were occupied by approximately two molecules of methyl viologen, and provided convincing arguments that the energy wasting back-electron transfer (BET) reaction between the redox partners of the initial photoproduct (i.e., $Ru(bpy)_3^{3+}/MV^{+\bullet}$) is retarded, to some extent, by the zeolite framework. In an impressive later report, these same workers showed that the reducing equivalents generated within the intrazeolitic space could be liberated by electron transfer to an excluded viologen of appropriate reduction potential, though the estimated quantum yields for production of extra-zeolitic acceptor were quite low, one of the reasons apparently being a persistent, relatively high rate of BET.[6c]

In view of the apparent promise such materials hold for catalysis and photocatalysis, efforts in this laboratory have been on the development of synthetic methods for elaboration of intrazeolitic catalytic assemblies.[7−9] Extending earlier work,[7] in which methods were devised to produce well-characterized zeolite-entrapped, tris-ligated, heteroleptic complexes, such as $Z\text{-}Ru(bpy)_2(bpz)^{2+}$ (where bpz is 2,2′-bipyrazine), we recently reported the successful preparation of strongly interacting dyads, wherein two ruthenium polypyridine complexes are situated in adjacent supercages.[8] Specifically, an adjacent cage dyad consisting of a $Ru(bpy)_2bpz^{2+}/Ru(mmb)_3^{2+}$ pair (where mmb is 5-methyl-2,2′-bipyridine) exhibited photophysical behavior consistent with the presence of an additional excited state decay pathway, which greatly reduced emission intensities and ^{3}MLCT excited-state lifetimes. Most significantly, upon selective excitation of the $Ru(bpy)_2bpz^{2+}$ complex, acting as a sensitizer, dramatically increased yields of excluded viologen radicals were observed, relative to an appropriate reference system, in an experimental arrangement similar to that used by Dutta and co-workers[6c] for the dyad system consisting of $Ru(bpy)_3^{2+}/DQ^{2+}$. The essential difference in the two systems is the presence of the adjacent cage $Ru(mmb)_3^{2+}$, which is of the appropriate reduction potential to serve as a potential donor to the oxidized sensitizer, $Ru(bpy)_2bpz^{3+}$, as is illustrated below.

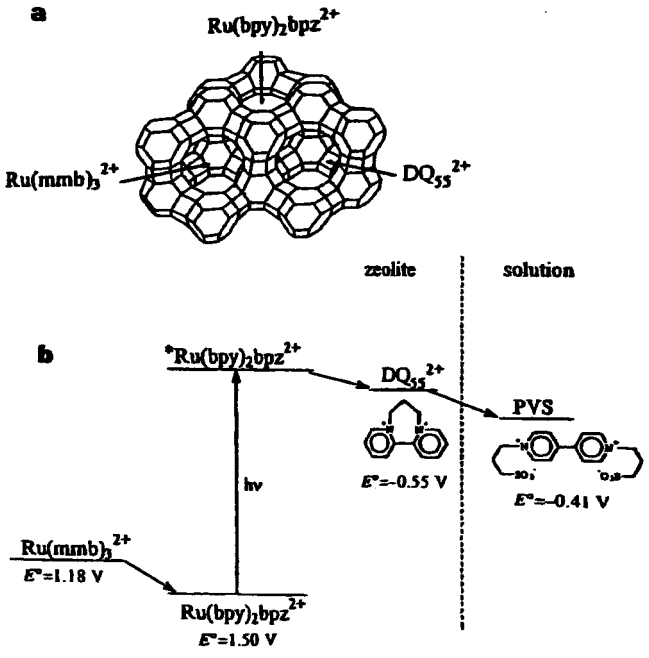

While the photophysical[8] and photoredox[9] experiments on the interesting system described above provided convincing indirect evidence for donor efficiency of the adjacent cage complex ($Ru(mmb)_3^{2+}$, above), attempts to definitively document the formation of $Ru(mmb)_3^{3+}$ are thwarted by side reactions which eventually lead to decomposition of the oxidized tris-ligated complex.[10] To more effectively address this issue, the present work was undertaken wherein the potential donor complex employed, $Ru(bpy)_2(H_2O)_2^{2+}$, is stable when oxidized. Spectroscopic and photophysical studies document the integrity of the intrazeolitic adjacent cage dyad and provide convincing evidence for an additional excited state decay pathway most reasonably attributable to electron-transfer quenching of the ^{3}MLCT excited state of the $Ru(bpy)_2bpz^{2+}$sensitizer.

Experimental Section

A. Materials. The Y-zeolite used in this study was generously provided by Union Carbide Corp. The crude zeolite was precleaned by oxidation under flow of oxygen at 500 °C for 5 hours[11] and extensively washed with a 10% NaCl solution and deionized water. Methyl viologen dichloride, $RuCl_3 \cdot 3H_2O$, $Ru(NH_3)_6Cl_3$ were purchased from the Aldrich Chemical Co and used without further purification. The ligand 2,2′-bipyridine (bpy) was obtained from Aldrich Chemical Co. and was sublimed prior to use. The ligand 2,2′-bipyrazine was prepared and purified following standard procedures.[12] $[Ru(NH_3)_5(H_2O)]^{2+}$ was prepared by literature methods.[13] All solvents used were reagent grade or better.

B. Preparation of Compounds. The zeolite-entrapped complexes $Z\text{-}Ru(bpy)_2(H_2O)_2^{2+}$ and $Z\text{-}Ru(bpy)_2(bpz)^{2+}$ were prepared by a modification of a method previously developed in our laboratory[7b] which are based on pioneering work of Lunsford and co-workers.[4] The precursor for the adjacent cage assembly, $Z\text{-}Ru(bpy)_2(bpz)\text{-}Ru(NH_3)_5$, was prepared by a method developed in our laboratory[8] which is the modification of the procedure reported for the preparation of $[Ru(bpz)_3 \cdot Ru(NH_3)_5](PF_6)_2$ in solution.[14] The adjacent cage assembly $Z\text{-}[Ru(bpy)_2bpz] \cdot [Ru(bpy)_2(H_2O)_2^{2+}]$ was prepared from the precursor material by the following procedure. Typically 0.5 g of $Z\text{-}Ru(bpy)_2bpz\text{-}Ru(NH_3)_5$ (1 complex per 60 supercages) and a 100 fold excess (relative to $Ru(bpy)_2bpz\text{-}Ru(NH_3)_5$) of bpy (i.e, 1.8 bpy per supercage) was suspended in 2 mL of 95% ethanol and stirred in 2 × 10 cm Pyrex tube overnight. The ethanol was evaporated under a stream of nitrogen. Next, the tube was alternately filled with nitrogen and evacuated three times. The evacuated tube was then immersed in a room temperature oil bath which was then slowly warmed to 90 °C. During this time the color of the sample slowly changed from blue to light pink indicating decomposition of the binuclear complex and formation of entrapped $Ru(bpy)_2(H_2O)_2^{2+}$. The heating at 90 °C was then continued for an additional 18 h and the sample was allowed to cool to room temperature. The product was washed with 1L of 10% aqueous NaCl, 200 mL of DI water and 200 mL of ethanol and then extensively (∼15 days) Soxhlet extracted with 95% ethanol to remove the excess ligand (the ultraviolet absorption spectrum of the ethanol washing was checked for the presence of excess ligand). Finally the product was air-dried. The zeolite-entrapped complex was extracted from the zeolite matrix by the hydrofluoric acid method described in ref 7a. The integrity of the zeolite-entrapped sample was confirmed by the spectroscopic measurements.

(7) (a) Maruszewski, K.; Strommen, D. P.; Handrich, K.; Kincaid, J. R. *Inorg. Chem.* **1991**, *30*, 4595. (b) Maruszewski, K.; Strommen, D. P.; Kincaid, J. R. *J. Am. Chem. Soc.* **1993**, *115*, 8345. (c) Maruszewski, K.; Kincaid, J. R. *Inorg. Chem.* **1995**, *34*, 2002. (d) Szulbinski, W. S.; Kincaid, J. R. *Inorg. Chem.* **1998**, *37*, 859. (e) Bhuiyan, A. A.; Kincaid, J. R. *Inorg. Chem.* **1998**, *37*, 2525. (f) Kincaid, J. R. *Chemistry: A European Journal* **2000**, *6*, 4055.
(8) Sykora, M.; Maruszewski, K.; Treffert-Ziemelis, S. M.; Kincaid, J. R. *J. Am. Chem. Soc.* **1998**, *120*, 3490.
(9) Sykora, M.; Kincaid, J. R. *Nature* **1997**, *387*, 162.
(10) Ledney, M.; Dutta, P. K. *J. Am. Chem. Soc.* **1995**, *117*, 7687.
(11) Incavo, J. A.; Dutta P. K. *J. Phys. Chem.* **1990**, *94*, 3075.
(12) Crutchley, R. J.; Lever, A. B. P. *Inorg. Chem.* **1982**, *21*, 2276.
(13) (a) Vogt, L. H.; Katz, J. L.; Wiberley, S. E. *Inorg. Chem.* **1965**, *4*, 1157. (b) Kuehn, C. G.; Taube, H. J. *J. Am. Chem. Soc.* **1976**, *98*, 689.
(14) Toma, H. E.; Auburn, P. R.; Dodsworth, E. S.; Golovin, M. N.; Lever, A. B. P. *Inorg. Chem.* **1987**, *26*, 4257.

C. Spectroscopic Measurements. 1. Electronic Absorption Spectra. Electronic absorption spectra of solutions were obtained with a Hewlett-Packard Model 8452A diode array spectrometer using a 1-cm quartz cuvette. Spectra were obtained in the absorbance mode. The diffuse reflectance spectra were recorded on Perkin-Elmer Model 320 spectrometer equipped with a Hitachi integrating sphere attachment. For these measurements, the zeolite samples were measured as KBr pellets and a plain Na−Y-zeolite sample was used as a blank. Finely ground $BaSO_4$ was used as a reference. The spectra were recorded in the transmittance mode and then numerically Kubelka−Munk[15] corrected using the facilities of SpectraCalc software.

2. Electronic Emission Spectra. Electronic emission spectra were obtained with a Spex model 1403 double monochromator equipped with a Spex model DM1B controller and Hammamatsu R928 photomultiplier tube. The excitation line (488.0 nm) was obtained from a Spectra-Physics Model 2025-05 argon ion laser. Zeolite-entrapped complexes were transferred into 5 mm i.d. NMR tubes and degassed overnight at $\sim 10^{-4}$ Torr and then exposed to the vapors of degassed (3 × freeze−pump−thaw) deionized water. The samples were finally sealed inside the NMR tube on the vacuum line. Spectra of the zeolite-entrapped complexes were obtained from a water suspension in rotating NMR tubes. The NMR tube was illuminated by a laser beam focused through a glass lens (laser power ~5mW at the sample) and the emission from the sample was collected with a conventional two-lens collection system. The laser was used in the constant power mode to avoid fluctuations of the excitation power during the measurements.

3. Resonance Raman Spectra. Resonance Raman spectra were obtained by using the same instrumental setup as described for the electronic emission spectra, using the 488.0 nm excitation line (laser power ~20mW at the sample) from the argon ion laser. Spectra of the zeolite-entrapped compounds were obtained from solid samples in rotating NMR tubes.

4. Excited-State Lifetimes. The samples for lifetime measurement were freshly degassed by the same procedure as described for emission measurements. The third harmonic (354.7 nm) of a Spectra-Physics Model GCR-11 Nd:YAG laser (operated at 20 Hz), with the beam defocused, was used as the excitation source for the lifetime measurements. The emitted light from the sample was transferred through collecting and transferring lenses to a Spex 340S spectrometer equipped with an RCA C31034A-02 photomultiplier tube with an applied voltage of 1800V. The photomultiplier tube output signal was directed to a Lecroy 9450 A dual 300-MHz oscilloscope. The emission was monitored at 670 nm in all cases. For all samples, 3000 scans of the emission decay curves were averaged and transferred to the computer. These curves were then fitted to a biexponential or triexponential model using commercial software (PSI-Plot). The quality of the fit for a particular model was monitored by comparing plots of the residuals between the experimental and the fitted curve. The number of exponential terms was changed until the residual values were below 2% and symmetrically distributed around the zero value.[19]

5. Solid State Photoredox Measurement. Methyl viologen dichloride was ion exchanged into zeolite containing the adjacent cage assembly for photoredox measurements. For the ion exchange step, typically 0.5 g of purified adjacent cage sample and 0.5 g of $MVCl_2$ were taken in a flask with 19 mL of deionized water (resulting in a 0.1 M solution of $MVCl_2$). The suspension was stirred overnight, then filtered and air-dried. The overall concentration of methyl viologen is two MV^{2+} per supercage.[6b] The dry sample was then transferred to a glass spectroscopic cell and the cell was connected to the vacuum line. The sample was then evacuated at $\sim 10^{-4}$ Torr overnight and the cell was sealed under vacuum. All steps described above were performed in the dark in order to avoid uncontrolled interaction between excited

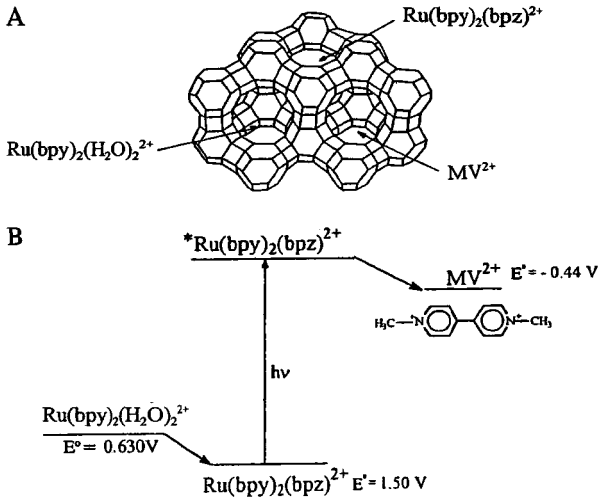

Figure 1. (A) Schematic diagram showing the arrangement of the donor ($Ru(bpy)_2(H_2O)_2^{2+}$); sensitizer ($Ru(bpy)_2(bpz)^{2+}$); acceptor (MV^{2+}) photocatalytic assembly. (B) Electron-transfer processes occurring inside the Y-zeolite particle on exposure to visible light.

complex and MV^{2+}. The sample sealed in the spectroscopic cell was irradiated with 457.9 nm laser line from an argon ion laser. The beam was defocused in order to irradiate the entire surface of the cell. The power of the beam, measured at the focal point (i.e., before the sample cell) was 100 mW. The sample was irradiated in 10 min intervals for 2 h and the formation of $MV^{+\bullet}$ was monitored by diffuse reflectance spectroscopy. A plain Na−Y-zeolite sample was used as a blank and finely ground $BaSO_4$ as a reference. The spectra were then Kubelka−Munk[15] corrected using SpectraCalc software.

Results and Discussion

A. Electronic Absorption Spectra. The diffuse reflectance spectrum of zeolite-entrapped Z-$Ru(bpy)_2(H_2O)_2^{2+}$ complex is shown in Figure 2C along with the absorption spectra of relevant complexes. The absorption spectrum of the free complex in water solution (trace A), as well as the liberated complex which is obtained following dissolution of the zeolite matrix (trace B), is virtually identical to the diffuse reflectance spectrum of Z-$Ru(bpy)_2(H_2O)_2^{2+}$. The spectra also match those reported in the literature,[7a,16] which confirm the formation of Z-$Ru(bpy)_2(H_2O)_2^{2+}$ species.

The diffuse reflectance spectrum of Z-$Ru(bpy)_2(bpz)^{2+}$ (trace C, Figure 3) is virtually identical to the absorption spectrum of the free complex in water solution (trace A, Figure 3). The absorption spectrum of the liberated complex after dissolution of the zeolite matrix (trace B, Figure 3) shows no significant differences in position of the absorption maxima compared to the spectrum of the free complex in water solution. The absorption spectrum of the free complex (trace A) matches that previously reported.[17] The absorption spectra consist of a series of absorption bands in the UV and visible region. The UV bands are ascribable to the ligand centered $\pi-\pi^*$ transition.[17] The visible bands are assigned to $d-\pi^*$ MLCT transitions.[17] The lower energy band is assigned to Ru→bpz and the higher energy one is ascribable to a Ru→bpy transition.[17]

The diffuse reflectance spectrum of Z-$Ru(bpy)_2(bpz)$-$Ru(NH_3)_5^{4+}$ sample is shown in Figure 4 along with the absorption spectra of relevant complexes. The spectra are similar to that previously reported for this material[8] and with that reported for $Ru(bpz)_3-Ru(NH_3)_5^{4+}$ by Crutchley and Lever[12] confirming the addition of a $Ru(NH_3)_5^{2+}$ fragment to the peripheral nitrogen of bpz. This attachment is indicated by the appearance of a new broad absorption band appearing near 650 nm. This band is

(15) Kubelka, P. *J. Opt. Soc. Am.* **1948**, *38*, 448.
(16) Sprintschnik, G.; Sprintschnik, H. W.; Krisch, P. P.; Whitten, D. G. *J. Am. Chem. Soc.* **1977**, *99*, 4947.
(17) Danzer, G.; Kincaid, J. R. *J. Phys. Chem.* **1990**, *94*, 3976.
(18) Rillema, D. P.; Jones, D. S.; Levy, H. A. *J. Chem. Soc., Chem. Commun.* **1979**, 849.
(19) (a) Sykora, M.; Kincaid, J. R.; Dutta, P. K.; Castagnola, N. B. *J. Phys. Chem.* **1999**, *103*, 309. (b) Allen, G. H.; White, R. P.; Rillema, D. P.; Meyer, T. J. *J. Am. Chem. Soc.* **1984**, *106*, 2613.

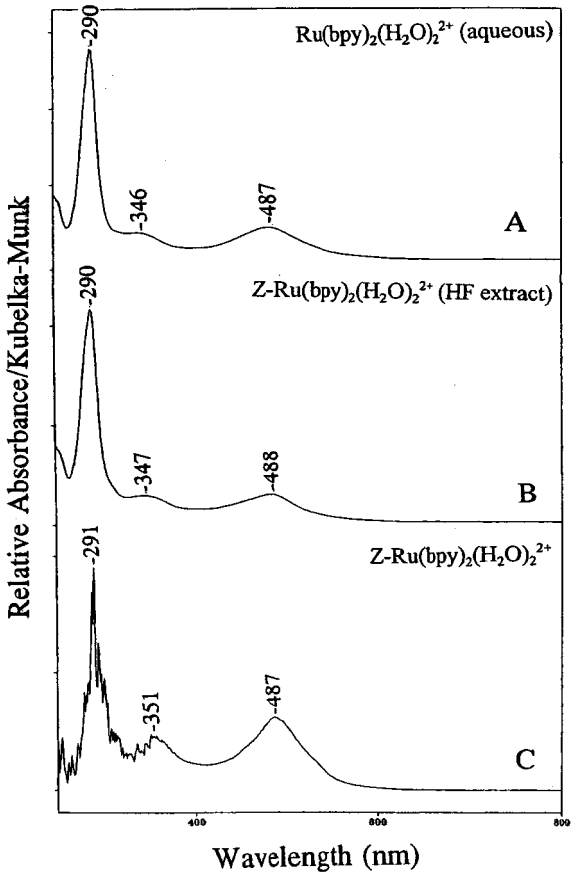

Figure 2. Electronic absorption spectra of $Ru(bpy)_2(H_2O)_2^{2+}$ free complex (trace A), extracted from zeolite matrix (trace B), and diffuse reflectance spectrum of zeolite entrapped complex (trace C).

ascribable to the metal-to-ligand charge transfer transition from the externally coordinated ruthenium pentaamine fragment.[8,12] The absorption spectrum of the liberated complex after dissolution of the zeolite matrix (trace B) is similar to the spectrum of the free complex in water solution (trace C, from ref 8), the very slight difference being attributable to small differences in solution composition and pH. This indicates that only one of the peripheral nitrogens of coordinated bipyrazine reacts with $Ru(NH_3)_5(H_2O)^{2+}$ to form Z-$Ru(bpy)_2(bpz)$-$Ru(NH_3)_5$. The other nitrogen of bipyrazine may not be accessible to the $Ru(NH_3)_5(H_2O)^{2+}$ ion or the reaction is disfavored owing to electrostatic factors. The size of the mononuclear complex $Ru(bpy)_2bpz^{2+}$ is ~12 Å[18] and the size of a supercage is ~13 Å. So the binuclear complex Z-$Ru(bpy)_2$bpz-$Ru(NH_3)_5$ is not likely to be accommodated in a single supercage, but rather, the peripheral nitrogen and the externally coordinated fragment $-Ru(NH_3)_5$ most likely extends into the neighboring supercage through the ~7 Å window opening.

The metalated intrazeolite complex Z-[$Ru(bpy)_2$bpz-$Ru(NH_3)_5$]$^{4+}$ is treated with an excess of bipyridine ligand at 90 °C to produce the desired adjacent cage assembly within the zeolite framework. The color changed from light blue to light pink which indicates the rupturing of the peripheral $N_{bpz}-Ru(NH_3)_5$ bond of the binuclear complex and the formation of two entrapped complexes in neighboring supercages. The diffuse reflectance spectrum of the product is shown in Figure 5 along with the absorption spectrum of the liberated complex after dissolution of the zeolite matrix (trace B). The disappearance of the band ~650 nm is associated with the rupture of the peripheral bond and the appearance of the 486 nm band is associated with the formation of Z-$Ru(bpy)_2(H_2O)_2^{2+}$.

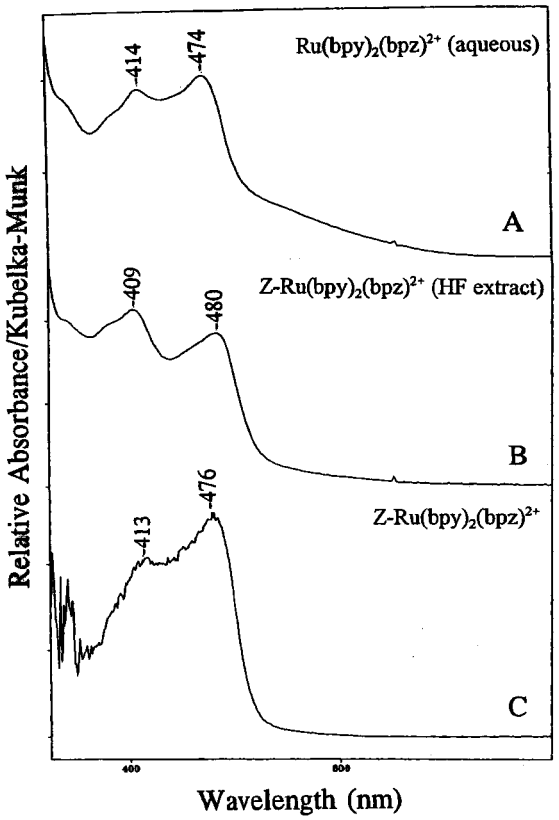

Figure 3. Electronic absorption spectra of $Ru(bpy)_2(bpz)^{2+}$ free complex (trace A), extracted from zeolite matrix (trace B), and diffuse reflectance spectrum of zeolite entrapped complex (trace C).

B. Resonance Raman (RR) Spectra. The RR spectra of the series of zeolite-entrapped complexes are shown in Figure 6. The frequencies of Z-$Ru(bpy)_2(bpz)^{2+}$ (trace C) and Z-$Ru(bpy)_2(H_2O)_2^{2+}$ (trace D) complexes are in good agreement with the literature,[7a,8] a fact which confirms the integrity of the entrapped complexes. The spectra of a 1:1 mechanical mixture (MM) (trace B) and the adjacent cage (AC) assembly (trace A) consist of bipyridine vibrations as well as bipyrazine vibrations. The frequencies and the relative intensities of the peaks are shown in Table 1. The main purpose of the RR measurements is to determine the relative abundance of the two complexes in the AC assembly. The mechanical mixture was prepared by mixing 1 part Z-$Ru(bpy)_2(bpz)^{2+}$ (1 complex ~30 cages) and 1 part Z-$Ru(bpy)_2(H_2O)_2^{2+}$ (1 complex ~30 cages). The RR spectra of the MM and the AC assembly are essentially identical in terms of peak positions and the peak intensities (Table 1).

C. Electronic Emission Spectra. The room-temperature emission spectra of a series of zeolite-entrapped complexes are shown in Figure 7. For these spectra, an excitation line at 488 nm was used for all samples. The emission spectrum of the zeolite-entrapped Z-$Ru(bpy)_2(bpz)^{2+}$ complex shows a strong emission band with a maximum ~670 nm which is in good agreement with the previously reported spectrum.[7b] The pure bis complex, Z-$Ru(bpy)_2(H_2O)_2^{2+}$, does not emit strongly at room temperature. The slight luminescence (~610 nm) of this sample results from the presence of a trace amount (<1%) of tris-ligated species, Z-$Ru(bpy)_3^{2+}$. The sample of zeolite-entrapped bis-bipyridine complex used here contained less than 1% of the tris complex impurity, as determined with emission spectroscopy by spiking the samples of Z-$Ru(bpy)_2(H_2O)_2^{2+}$ with small (known) amounts of Z-$Ru(bpy)_3^{2+}$. The adjacent cage complex also contains less than 1% Z-$Ru(bpy)_3^{2+}$ impurity as determined by the same procedure.

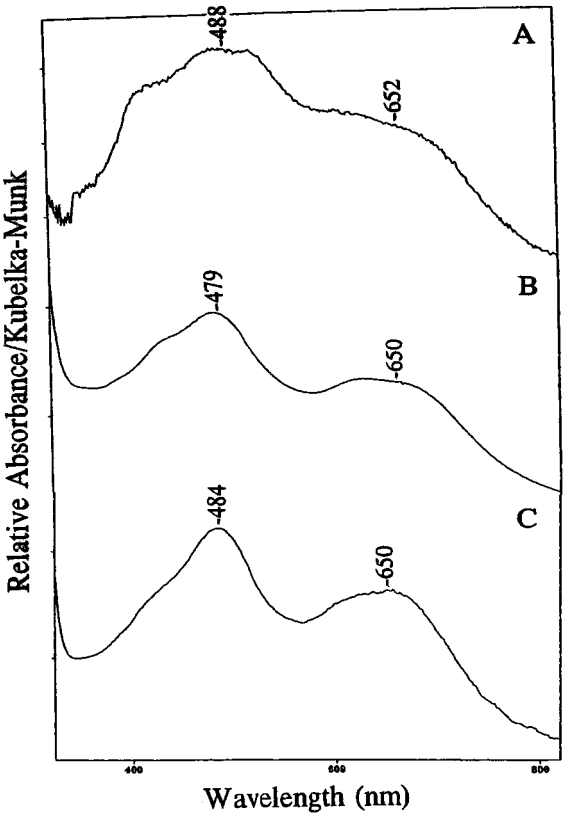

Figure 4. Diffuse reflectance spectrum of Z-Ru(bpy)$_2$(bpz)-Ru(NH$_3$)$_5^{4+}$ (trace A), electronic absorption spectra after extraction from zeolite matrix (trace B), free complex (trace C, from ref 8).

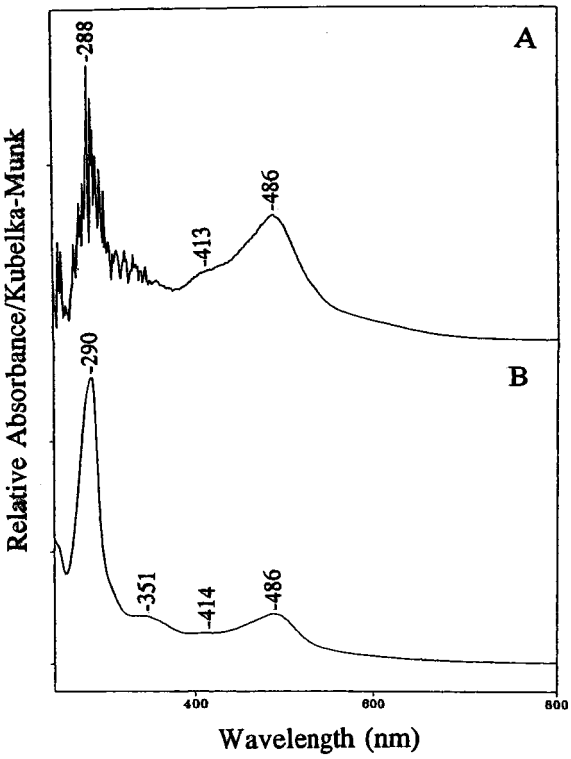

Figure 5. Diffuse reflectance spectrum of adjacent cage assembly, Z-[Ru(bpy)$_2$(bpz)·Ru(bpy)$_2$(H$_2$O)$_2$]$^{4+}$ (trace A), extracted from zeolite matrix (trace B).

The decrease in emission intensity of the sample of MM, which contains equal amounts of the two complexes, relative to the measured intensity of the sample of Z-Ru(bpy)$_2$bpz^{2+}, is

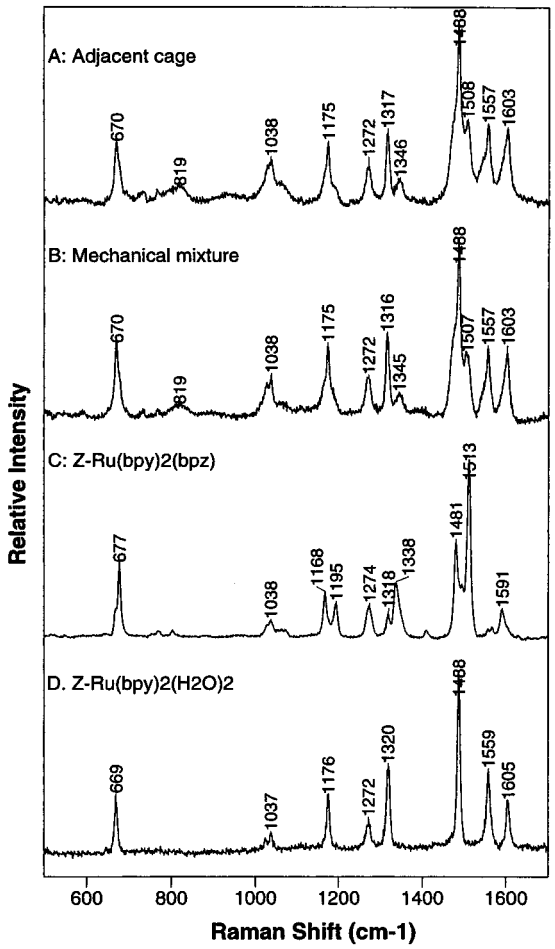

Figure 6. Resonance Raman spectra (with 488.0 nm excitation) of adjacent cage assembly (trace A), 1:1 mechanical mixture of Z-Ru(bpy)$_2$(bpz)$^{2+}$ and Z-Ru(bpy)$_2$(H$_2$O)$_2^{2+}$ (trace B), Z-Ru(bpy)$_2$(bpz)$^{2+}$ (trace C), and Z-Ru(bpy)$_2$(H$_2$O)$_2^{2+}$ (trace D). The relative concentrations of the complexes are same in all cases (1 complex per ~30 cages).

Table 1. Comparison of Resonance Raman Frequencies (cm^{-1}) and Relative Intensities[a] of Mechanical Mixture[b] (MM) and Adjacent Cage Assembly[c] (AC) with 488.0 nm Excitation

MM (cm^{-1})	intensity	AC (cm^{-1})	intensity
670	4.2	670	3.6
819	1.0	819	1.1
1038	2.5	1038	2.6
1175	4.1	1175	3.6
1272	2.4	1272	2.3
1316	4.7	1317	4.3
1345	1.5	1346	1.5
1488	10.0	1488	10.0
1507	4.0	1508	4.5
1557	4.2	1557	4.4
1603	3.9	1603	4.1

[a] Intensities on relative scale with 10.0 maximum. [b] Mechanical mixture (1:1), equal amounts of Z-Ru(bpy)$_2$(bpz)$^{2+}$ and Z-Ru(bpy)$_2$(H$_2$O)$_2^{2+}$. [c] Adjacent cage assembly Z-[Ru(bpy)$_2$(bpz)·Ru(bpy)$_2$(H$_2$O)$_2$]$^{4+}$.

attributable to the lower concentration of the emitter and to the decrease in effective incident power owing to the absorption of light by the nonemitting Ru(bpy)$_2$(H$_2$O)$_2^{2+}$ component. The most important observation in this set of emission data is the substantial decrease (53%) in emission intensity observed for the adjacent cage assembly, relative to the mechanical mixture. These two samples contain the same absolute amounts of the entrapped complexes, the only difference being in the spatial arrangement, which is therefore responsible for the dramatic

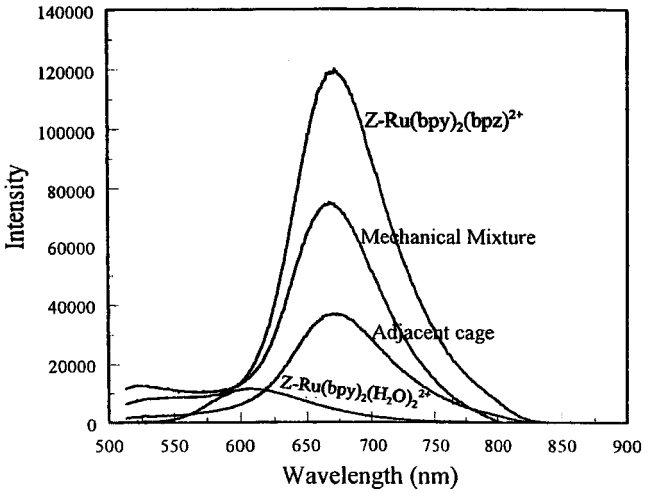

Figure 7. Electronic emission spectra for a series of zeolite entrapped complexes recorded with 488.0 nm excitation. The relative concentrations of the complexes are same in all cases (1 complex per ~30 cages).

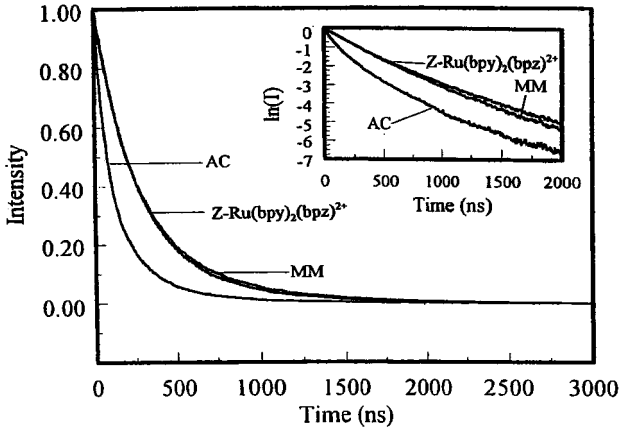

Figure 8. Emission decay curves for a series of zeolite entrapped complexes obtained at room temperature with 354.7 nm excitation. The concentrations are the same as in Figure 6. The insert presents the logarithmic plots for the same data.

decrease in emission intensity. In the mechanical mixture, each zeolite particle contains either $Ru(bpy)_2(bpz)^{2+}$ or $Ru(bpy)_2(H_2O)_2^{2+}$, so physical interaction between the complexes is not possible. In the case of adjacent cage assembly, the same zeolite particle contains both the complexes in adjacent supercages of zeolite, which is within the physical interaction distance. The dramatic decrease in the case of the adjacent cage assembly, relative to the mechanical mixture, is ascribable to the activation of an additional nonradiative decay pathway.[8,19a]

D. Excited-State Lifetimes. The decay curve of the adjacent cage assembly (AC), along with those obtained for the reference materials, were measured at room temperature and are shown in Figure 8. The emission was monitored at 670 nm for all the materials. The insert in Figure 8 presents the logarithmic plots for the same data. For the zeolite-entrapped complex, Z-$Ru(bpy)_2(bpz)^{2+}$, it was necessary to apply a biexponential model ($I = I_{01} \exp(-t/\tau_1) + I_{02} \exp(-t/\tau_2)$) of the decay to reproduce the observed decay curve, as in the case of other zeolite entrapped complexes.[2e,7b,c,e] The lifetime for the aqueous suspension of the zeolite entrapped $Ru(bpy)_2(bpz)^{2+}$ complex was ~228 ns (75%) with a second component (~470 ns) contributing approximately 25% of the initial emission intensities. The minor component is attributable to the small fraction (less than 1%) of Z-$Ru(bpy)_3^{2+}$ impurity and (possibly) a small contribution from interacting adjacent cage pairs.[19a] The minor component actually may represent an averaged contribution of Z-$Ru(bpy)_3^{2+}$ and adjacent cage pairs. The individual components cannot be resolved during the numerical fitting because of their small relative contributions to the emission decay.

Comparison of the traces in Figure 8 and Table 2 indicates that the emission decays of Z-$Ru(bpy)_2(bpz)^{2+}$ and the mechanical mixture are comparable to each other but the emission decay of the adjacent case assembly is much more rapid. This observation is consistent with the decrease in emission intensity mentioned in the previous section. The curve observed for the mechanical mixture is very similar to Z-$Ru(bpy)_2(bpz)^{2+}$, as expected, because the other component of the mechanical mixture, Z-$Ru(bpy)_2(H_2O)_2^{2+}$, does not emit at room temperature and there is no interaction between the complexes. However, for the adjacent cage assembly, the decay curve is quite different from that of the mechanical mixture. In the former case, it was necessary to apply a triexponential model ($I = I_{01} \exp(-t/\tau_1) + I_{02} \exp(-t/\tau_2) + I_{03} \exp(-t/\tau_3)$) of the decay to reproduce the observed decay curve. The results are shown in Table 2. There is a very short-lived component ($\tau_3 = 58$ ns) that dominates the decay curve at early time and at longer time (above ~100 ns) the decay behavior is quite similar to that of the mechanical mixture. Inasmuch as there is no evidence for such a short-lived ($\tau_3 = 58$ ns) component for the MM sample, this short component is most reasonably attributed to interactions within the adjacent cage dyads. The analysis of the lifetime data for the adjacent cage assembly indicates that the short component contributes approximately 50% of the total emission intensities, which means 50% of the excited-state population decays by this rapid process.

It is interesting to consider various possible decay mechanisms which might give rise to this short component. Several quenching mechanisms by which the two components of the adjacent cage dyad might interact and depopulate the excited state are summarized below with estimated energetics.

1. Oxidative electron transfer:

$$*Ru(bpy)_2(bpz)^{2+} + Ru(bpy)_2(H_2O)_2^{2+} \rightarrow Ru(bpy)_2(bpz)^{3+} + Ru(bpy)_2(H_2O)_2^{+} \qquad \Delta G^\circ = 0.61 \text{ eV}$$

2. Reductive electron transfer:

$$*Ru(bpy)_2(bpz)^{2+} + Ru(bpy)_2(H_2O)_2^{2+} \rightarrow Ru(bpy)_2(bpz)^{+} + Ru(bpy)_2(H_2O)_2^{3+} \qquad \Delta G^\circ = -0.42 \text{ eV}$$

3. Energy transfer:

$$*Ru(bpy)_2(bpz)^{2+} + Ru(bpy)_2(H_2O)_2^{2+} \rightarrow Ru(bpy)_2(bpz)^{2+} + *Ru(bpy)_2(H_2O)_2^{2+} \qquad \Delta G^\circ = 0.06 \text{ eV}$$

$$*Ru(bpy)_2(H_2O)_2^{2+} \rightarrow Ru(bpy)_2(H_2O)_2^{2+} + \text{heat (nonradiative decay)}$$

The listed ΔG° values are calculated by using the reported values of the ground and excited-state redox potentials listed in ref 5c. From the above mechanisms it is clear that the reductive electron-transfer quenching process is an energetically favorable process. These types of estimates yield crude approximations for ΔG°, since ground and excited state redox potentials for the zeolite entrapped complexes are not available. The essential point here is that a strong interaction between the components of adjacent cages is clearly documented from this

Table 2. Excited State Lifetimes (ns) for Adjacent Cage Assembly and Related Complexes

compound	τ_1 (I_{01})[c]	τ_2 (I_{02})[c]	τ_3 (I_{03})[c]
Z-Ru(bpy)$_2$(bpz)$^{2+}$	228 (75)	470 (25)	
Ru(bpy)$_2$(bpz)$^{2+}$ (H_2O)[d]	127 (100)		
Ru(bpy)$_2$(bpz)$^{2+}$ (PC)[e]	353 (100)		
MM[a]	199 (62)	468 (38)	
AC[b]	187 (40)	470 (10)	58 (50)

[a] Mechanical mixture (1:1), equal amounts of Z-Ru(bpy)$_2$(bpz)$^{2+}$ and Z-Ru(bpy)$_2$(H_2O)$_2^{2+}$. [b] Adjacent cage assembly Z-[Ru(bpy)$_2$(bpz)·Ru(bpy)$_2$(H_2O)$_2$]$^{4+}$. [c] I_{oi} represents the relative contribution of the ith component to the total emission intensity. [d] Data from ref 7b. [e] Propylene carbonate, data from ref 19b.

study; behavior which is consistent with the previously reported results for a similar system.[8,19a]

E. Photoredox Study. The adjacent cage assembly was investigated with respect to its ability to mediate photoinduced electron transfer to methyl viologen cation (MV^{2+}) loaded into the remaining supercages of the zeolite particles. This study is analogous to studies conducted by Dutta and co-workers[6b,c] for systems containing only S/A dyads and by Sykora and Kincaid[9] on samples loaded with Z-[Ru(bpy)$_2$(bpz)$^{2+}$/Ru(mmb)$_3^{2+}$]/DQ^{2+}/PVS; i.e., wherein A/S/D triads were generated. While the results of these comparative studies of net-charge separation efficiency documented a substantial improvement of the triad system over the simpler systems,[9] most reasonably attributable to efficient reduction of the oxidized sensitizer of the initial (S^+/A^-) photoproduct, the instability[10] of the oxidized donor of that system prevented direct confirmation of its appearance. The present study was undertaken in order to produce a system wherein the production of the oxidized donor could be directly established; i.e., the assembly, Z-[Ru(bpy)$_2$(bpz)$^{2+}$/Ru(bpy)$_2$(H_2O)$_2^{2+}$/MV^{2+}.

The formation of methyl viologen radical ($MV^{+\bullet}$) upon irradiation with laser light is indicated by a blue color of the sample and was confirmed by diffuse reflectance spectroscopy. Figure 9A shows the formation of methyl viologen radical cation ($MV^{+\bullet}$) by the appearance of the characteristic absorption bands.[6c,9,20] of $MV^{+\bullet}$ at ~398 nm and ~607 nm, which are observed to grow in with irradiation time. Figure 9B shows the difference spectra which were generated by subtracting the spectrum of the original sample (before irradiation) from the spectra at various times (after irradiation). The increase in the concentration of $MV^{+\bullet}$ as a function of irradiation time is clearly evident. Furthermore, the decrease in the intensity of an absorption band at ~489 nm, assignable to the MLCT transition of Ru(bpy)$_2$(H_2O)$_2^{2+}$, indicates the formation of Z-Ru(bpy)$_2$(H_2O)$_2^{3+}$. It is important to point out that in the system studied earlier, Z-[Ru(bpy)$_2$(bpz)$^{2+}$/Ru(mmb)$_3^{2+}$]/MV^{2+}, wherein the oxidized donor complex apparently undergoes rapid side reactions to regenerate the reduced Ru(mmb)$_3^{2+}$, no evidence for donor oxidation was obtained, in contrast to the case studied here. The magnitude of the growth of $MV^{+\bullet}$ for the adjacent cage assembly as a function of photolysis time is plotted in Figure 10 along with the growth profiles for the material containing an isolated sensitizer; i.e., Z-Ru(bpy)$_3^{2+}$. It is clearly evident from Figure 10 that the efficiency of the radical formation of the adjacent cage assembly is much higher (approximately 4 times) than the isolated sensitizer with respect to net charge separation. This increased efficiency is directly attributable to the unique spatial organization of the two complexes.

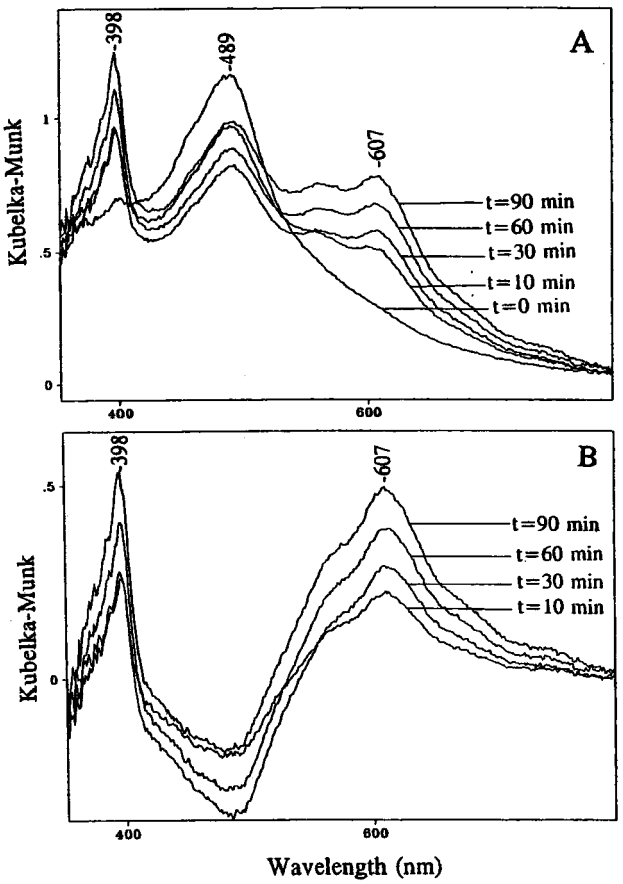

Figure 9. (A) Changes in the diffuse reflectance spectra upon irradiation of 100 mW of 457.9 nm laser line on methyl viologen loaded adjacent cage assembly, Z-[Ru(bpy)$_2$(bpz)·Ru(bpy)$_2$(H_2O)$_2$]$^{4+}$/MV^{2+}. (B) The difference spectra were generated by subtracting the original spectra (before irradiation) from the spectra at various time (after irradiation).

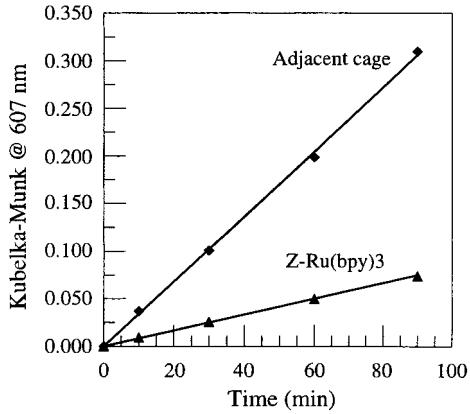

Figure 10. Growth of $MV^{+\bullet}$ as a function of photolysis time for the adjacent cage dyad assembly, Z-[Ru(bpy)$_2$(bpz)·Ru(bpy)$_2$(H_2O)$_2$]$^{4+}$ (AC), and for the isolated system, Z-Ru(bpy)$_3^{2+}$. In both cases the relative concentrations of the complexes are same (1 complex per ~30 cages). The calculated slopes are as follows: 3.40×10^{-3} min^{-1} (AC) and 0.82×10^{-3} min^{-1} (Z-Ru(bpy)$_3^{2+}$).

Conclusions

The present study addresses an important issue regarding the functional properties of zeolite-based organized molecular

(20) (a) Alam, M. M.; Ito, O. *J. Phys. Chem.* **1999**, *103*, 1306. (b) Kim, Y. S.; McNiven, S.; Ikebukuro, K.; Karube, I. *Photochem. Photobiol.* **1997**, *66*, 180. (c) Takuma, K.; Kajiwara, M.; Matsuo, T. *Chem. Lett.* **1977**, 1199. (d) Kalyanasundaram, K.; Dung, D. *J. Phys. Chem.* **1980**, *84*, 2402. (e) Watanabe, T.; Honda, K. *J. Phys. Chem.* **1982**, *86*, 2617.

assemblies, an important class of materials, which have been shown previously[9] to enhance net charge separation efficiency in zeolite-based photochemical systems.[6c] The work presented here describes a successful modification of previously developed synthetic procedures to permit incorporation of more attractive donor components into such assemblies. Spectroscopic characterization of the zeolite-entrapped components, both within the zeolite matrix and upon liberation into aqueous solution, confirms the integrity of the individual components as well as the expected relative concentrations within the particles. Emission spectra and lifetime measurements document a strong interaction between the adjacent cage pairs, indicating that the $Ru(bpy)_2(H_2O)_2^{2+}$ complex is appropriately positioned to function as a donor. The observed decrease in absorption bands of the donor complex, coupled with a dramatic increase in $MV^{+\bullet}$ formation, upon irradiation of a sample of the adjacent cage dyad system which has been loaded with the methyl viologen acceptor, provides direct evidence that BET is decreased by virtue of the fact that the oxidized sensitizer $[Ru(bpy)_2bpz^{3+}]$- of the initial photoproduct $[S^+/A^-]$ is efficiently reduced by the adjacent cage $Ru(bpy)_2(H_2O)_2^{2+}$ donor complex, thus confirming the targeted synergy of the assembly.

Acknowledgment. This work was supported by a grant from the Division of Chemical Sciences, U.S. Department of Energy (Grant DE-FG02-86ER 13619). The authors express their sincere thanks to Dr. Milan Sykora for helpful discussions and for providing the data for the photoredox study of the Z-$Ru(bpy)_3^{2+}$ sample.

IC010191M